15th International Particle Accelerator Conference,Nashville, TN JACoW Publishing
ISBN: 978-3-95450-247-9 ISSN: 2673-5490 doi: 10.18429/JACoW-IPAC2024-THPR22

STATUS OF THE BONN ISOCHRONOUS CYCLOTRON

D. Sauerland*, R. Beck, S. Birkenbach, S. Dernbach, A. Henny, B. Kann, M. Klümpen, M. Loepke, E. Momper, C. Noll, Helmholtz-Institut für Strahlen- und Kernphysik, Bonn, Germany
P. Wolf, Silizium Labor Bonn, Physikalisches Institut, Bonn, Germany

Abstract

The Bonn Isochronous Cyclotron provides proton, deuteron, alpha and other light ion beams with a charge-to-mass ratio $Q/A \geq 1/2$ and kinetic energies ranging from 7 to 14 MeV per nucleon. The beam is guided through a high-energy beam line (HEBL) to one of five experimental sites. The installation of the irradiation site for high-uniformity radiation hardness tests of Si detectors is now complete. Additionally, a neutron irradiation site will be commissioned soon. Here, a collimated neutron beam, generated by a stripping reaction of the deuteron beam in a carbon target, can be used for irradiation. To provide stable beam with constant optics for these experiments, the power supplies (PS) of all magnets in the HEBL will be replaced. The replacements must meet strict criteria regarding output current's stability, which were derived from measurements of the existing PS. In this spirit, a new corrector magnet PS system, enabling bipolar operation, PS/magnet operation safety/health and power consumption monitoring, is close to commissioning. Additionally, the cyclotron's extraction septum is upgraded to increase operation robustness. Here, an new antiseptum is designed together with a new septum blade holder, which is intended to be additively manufactured with the laser-powder bed fusion technique.

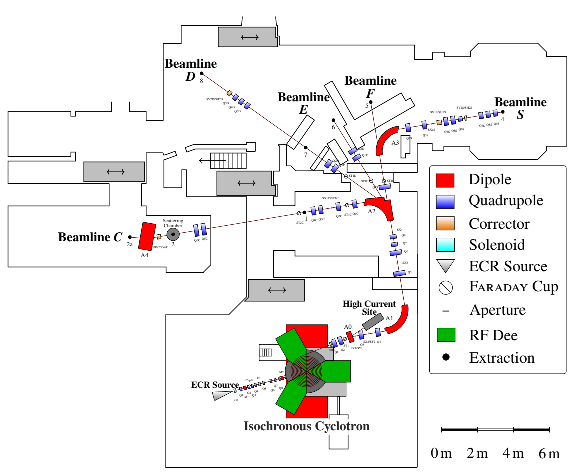

Figure 1: Overview of the accelerator facility.

BONN ISOCHRONOUS CYCLOTRON

In Fig. 1, the accelerator facility of the Bonn Isochronous cyclotron is shown. Here, five experimental sites are provided with light ions, like protons, deuterons or alpha particles with a kinetic energy of 7 to 14 MeV$/A$.

The ion beam is generated by two electron cyclotron resonance sources. The beam is directed through a low-energy beamline below the cyclotron and then is injected vertically into its magnetic center using an electrostatic hyperboloid inflector.

The Bonn Isochronous Cyclotron is an isochronous, three-sector, azimuthally varying field cyclotron. The cyclotron shows a 120°-symmetry in its azimuthal magnetic field pattern due to its magnet yoke being separated into three hill-and-valley sectors with 0° spiral angle. In each valley, a broadband dual-gap dee is located, providing an acceleration voltage of up to 40 kV. The beam is extracted to a field-compensated channel in a single-turn extraction, using an electrostatic septum. The extracted beam can either be guided to the high current site, used to produce induced radioactivity in target material, or it is transported to the experimental sites via the high-energy beamline.

RECENT DEVELOPMENTS

In 2023 and 2024, several sites and components were advanced or upgraded.

Proton Irradiation Site

The proton irradiation site at beamline C (comp. Fig. 1) for high-homogeneity radiation hardness tests of Si detectors is discussed in detail amongst others in [1] and [2].

By determining the proton hardness factor, the site now is completely characterized for the typical irradiation beam energy of 13.6 MeV (12.3 MeV on the irradiated device) [1]. Here, six 150 µm-thick, $(1.92 \times 0.96)\,\mathrm{cm}^2$, passive sensors from LFoundry are irradiated to fluences ranging from 5×10^{12} to 1.6×10^{14} protons cm^{-2}. After annealing for 80 min at 60 °C, their leakage current at full depletion is determined. From the increase in leakage current per depleted volume with increased proton fluence, the hardness factor is determined as $\kappa_\mathrm{p} = 3.71(11)$.

Neutron Irradiation Site

The facility's irradiation capabilities are extended by a neutron irradiation site at beamline F in future (see Fig. 2). Here, the deuteron beam passes a diagnostic section and impinges on a cylindrical 2.4 mm thick carbon converter, where a neutron beam is generated in a stripping reaction. Also generated protons are stopped in the converter whereas the neutrons pass through a subsequent 1.24 m long copper collimator with tungsten inlets. The 24 inlets with an individual length of 5 cm have the form of cylinders with conical centric holes of different sizes. The overall geometry of the lined-up inlets has the form of a double-conical hole with 3 cm-diameter entry, 1 cm-diameter constriction after 15 cm

* sauerland@hiskp.uni-bonn.de

ISBN: 978-3-95450-247-9 ISSN: 2673-5490 doi: 10.18429/JACoW-IPAC2024-THPR22

Table 1: Results of the stability measurements of HEBL dipole and quadrupole magnet PS. Note that the manufacturer states the DCCT's accuracy as $< 3 \times 10^{-5}$/Full Scale and $< 2 \times 10^{-6}$/°C with $\Delta T \approx 4$ °C during the measurements.

	Cyclotron Magnet	**A1**	**A2/A3**	**Q1**	**Q2**	**Q3**	**Q4C**	**Q5**	**Q6**	**Q7**
I_{RMS} / $\langle I \rangle$ / 10^{-5}	1.12	0.09	7.69	2.41	12.82	2.84	2.15	3.05	6.30	0.42
Duration / h	24	4	4	4	4	3.5	4	2	3	2
Sampling rate / Hz	0.1	1	1	1	1	1	1	1	1	1

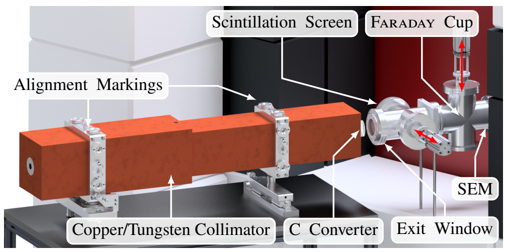

Figure 2: CAD render of the neutron beam generation setup at beamline F with mock converter.

and a 3 cm-diameter exit. Here, the neutron beam is shaped towards a homogeneous 3 cm-diameter beamspot after the collimator with a broad energy spectrum around an average energy of ≈ 8 MeV, as seen in `geant4` simulations.

The applied neutron fluence is directly proportional to the integrated deuteron beam current. Therefore, a secondary electron monitor (SEM) is installed in the diagnostic section upstream of the neutron beam generation (see Fig. 3). The SEM is similar to one, used in the beamline C (comp. [2]), with horizontally (SEM U & D) and vertically (SEM L & R) segmented 5 µm thick, carbon-coated Al foils with surrounding pull electrodes (+100 V). This design allows for non-destructive measurement of the beam current as well as its position. For SEM-calibration, a retractable Faraday cup, featuring an inverted cone shape with an upstream suppressor electrode (−100 V) for maximal charge collection efficiency, is included after the SEM. A retractable *Chromox* scintillation screen allows for visual beam diagnostic.

In May 2024, the complete beam diagnostic section was commissioned and tested. After design and construction of the converter, in a next step the collimator will be equipped with newly manufactured inlets and it will be precisely aligned on the beam axis using a laser tracker. Then the generated neutron beam will be characterized using the techniques of N-γ discrimination and metalic foil activation.

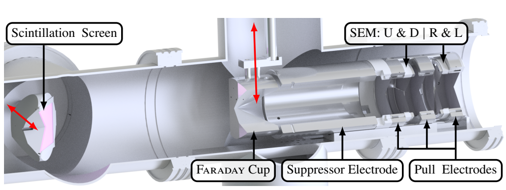

Figure 3: Sectional view of a CAD render of the diagnostic section with retractable Faraday cup and scintillation screen.

Modernization of Magnet Power Supplies

To provide a stable beam with constant machine optics for the experiments, the existing power supplies of all HEBL magnets will be replaced by modern PS in future. These PS will be integrated into modern Programmable Logic Controller (PLC) Systems and will be controlled by the upcoming cyclotron control system.

In a first step towards PS modernization, the stability of most existing HEBL dipole and quadrupole magnet PS was studied by integrating a direct current-current transformer (DCCT) into the circuit between PS and magnet. The DCCT output is recorded for a duration of several hours. The stability is derived from the current's root mean square I_{RMS} devided by the average current $\langle I \rangle$ (see Table 1). After clarifying systematical errors in this study, the purchase of new PS with equal or better stability (along with other parameters), will be based on these results.

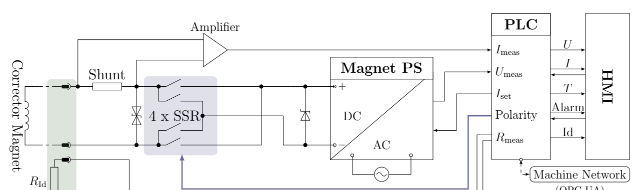

Figure 4: Schematic circuit diagramm of one corrector magnet power supply.

The first modernized component are the corrector magnet PS. Here, eight new PS (up to 24 A at 35 V) with a 8 h-stability of 9×10^{-5} in current control mode were purchased. All these PS will be controlled by one PLC in a system, schematically shown in Fig. 4. The system will be piloted by a human-machine interface (HMI), situated in the cyclotron's control room. In future also control by the control system via the OPC UA machine network will be possible. The PLC provides set current I_{set} to the individual PS and reads back the actual current, measured by a voltage drop over a shunt at the output. During zero-crossing of the output, the system is able to switch the output's polarity and thus current, using four solid-state relais (SSR). Each corrector magnet will be identified by the PLC with an individual resistor R_{Id}, which is integrated into in its connector, allowing to set safe operation parameters.

Upgrade of the Extraction Septum

The extraction septum is an electrostatic deflector, biased with up to −40 kV, which guides the beam into the extraction

ISBN: 978-3-95450-247-9 ISSN: 2673-5490 doi: 10.18429/JACoW-IPAC2024-THPR22

channel once the beam passes the septum blade (see Fig. 5). The 0.2 mm-thick tungsten blade is mounted onto two water-cooled blade holder, which acts as heat sink. The holders and the blade are on ground potential. On high-voltage potential, a water-cooled, copper antiseptum is located at a minimum distance of 4 mm to the blade. This distance is adjusted by altering the screw-in depth at the antiseptum's mounting points within two ceramic insulators. To prevent electric discharges between ground and high-voltage side, the electrodes' surface either show a mirror-finish (blade) or are chrome-plated (antiseptum) with rounded corners.

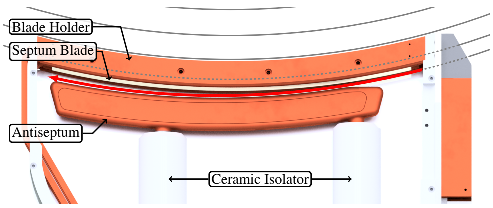

Figure 5: CAD render of the extraction septum with the new antiseptum design. The extracted beam is denoted in red.

New Antiseptum Design The previous design of the antiseptum required brazing twice: First the two antiseptums mounting points, which also comprised the water connections, had to be brazed onto the side of the antiseptum's body and then the cooling channels had to be braze-sealed with a cover plate on the body's top. Often leaks at the mounting points' brazing seams emerged due to mechanical stress during adjustment of the antiseptum's position. Therefore in the new design (see Fig. 5), the body and mounting points with water connections are milled from one single copper block using a 5-axis CNC milling machine. Only the cooling channels are braze-sealed with a cover. After overmilling the brazing seam on the cover, the antiseptum is hard chrome-plated and polished.

Additive-Manufactured Blade Holder The existing septum blade holder is a simple curved rectangle, milled from copper. The water cooling, an ensemble of soldered rectangular copper tubes, is screw-mounted onto it. Due the cooling's several leak-prone soldering seams and a reduced heat transfer from blade to water by the screw-mountings, a new blade holder, also comprising the water cooling, was designed (see Fig. 6). For production of this component, it is intended to use the pure-copper laser-powder bed fusion technique (L-PBF) [3] with subsequent heat-treatment (increases thermal conductivity κ and material strength) and polishing. The holder (128 g, 14.3 cm^3 volume) features a 4 mm-diameter water cooling channel at 1 mm distance from the septum blade and it is electrically isolated from the holder's supports to enable impinging-beam measurement for optimization of the septum's extraction efficiency.

To study the septum blade's equilibrium temperature and the cooling efficiency of the blade holders when in operation, simulations were conducted using the Thermal Steady

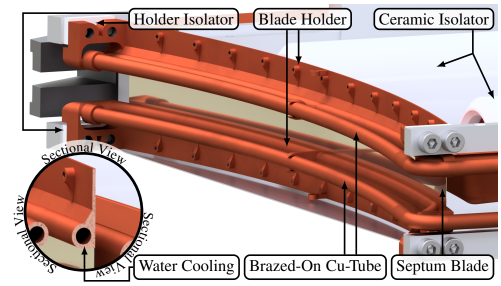

Figure 6: CAD render of the new blade holder, being integrated into the extraction septum (comp. Fig. 5).

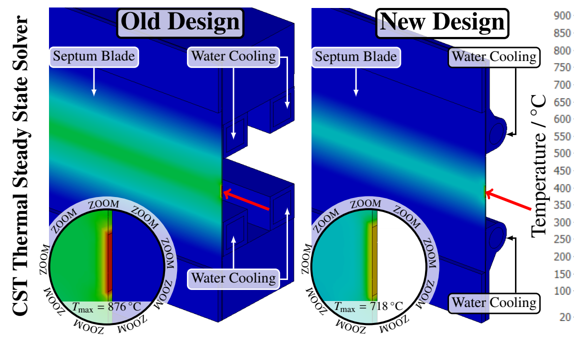

Figure 7: CST simulation of a 15 µA, 56 MeV α beam (red arrow) impinging on the edge (13 %P_0) and side (37 %P_0) of the septum blade with the old and new blade holder design.

State Solver of CST Studio Suite (see Fig. 7). Here, an α beam (total power P_0 = 840 W), hits the septum blade in a worst case scenario. Assuming perfect thermal contact of the components, the existing blade holder of copper (κ = 401 W m^{-1} K^{-1}) shows a maximal equilibrium temperature T_{max} of 876 °C at the blade's edge. The L-PBF-made blade holder (κ = 406 W m^{-1} K^{-1} [3]) by contrast showed a T_{max} of 718 °C. It can be assumed, that both T_{max} will be higher in reality due to finite thermal contact. However, the new design with ≈ 20 % better cooling efficiency, will be manufactured via L-PBF soon.

REFERENCES

[1] P. Wolf *et al.*, "A beam-driven proton irradiation setup for precision radiation damage tests of silicon detectors", *Nucl. Instrum. Meth. A*, vol. 1064, p. 169358, April 2024. doi:10.1016/j.nima.doi:2024.169358

[2] D. Sauerland *et al.*, "Proton Irradiation Site for High-Uniformity Radiation Hardness Tests of Silicon Detectors at the Bonn Isochronous Cyclotron", in *Proc. Cyclotrons'22*, Beijing, China, Dec. 2022, pp. 38-41. doi:10.18429/JACoW-CYCLOTRONS2022-MOBO03

[3] T. De Terris *et al.*, "Additive manufacturing of pure copper: a review and comparison of physical, microstructural, and mechanical properties of samples manufactured with Laser-Powder Bed Fusion (L-PBF), Electron Beam Melting (EBM) and Metal Fused Deposition Modelling (MFDM) technologies", *Inter. J. Mat. Forming*, vol. 16, no. 32, May 2023. doi:10.1007/s12289-023-01755-2